Magnetic moment orientations in alpha-Fe nanowire arrays embedded in anodic aluminum oxide templates

2002 J. Phys.: Condens. Matter 14 6875

(http://iopscience.iop.org/0953-8984/14/27/311)

INSTITUTE OF PHYSICS PUBLISHING JOURNAL OF PHYSICS: CONDENSED MATTER

J. Phys.: Condens. Matter **14** (2002) 6875–6882 PII: S0953-8984(02)36271-4

Magnetic moment orientations in α-Fe nanowire arrays embedded in anodic aluminum oxide templates

Fashen Li, Liyuan Ren[1], Ziping Niu, Haixin Wang and Tao Wang

Key Laboratory for Magnetism and Magnetic Materials of the Ministry of Education, Lanzhou University, Lanzhou 730000, People's Republic of China

E-mail: liyuanren@hotmail.com

Received 30 May 2002
Published 28 June 2002
Online at stacks.iop.org/JPhysCM/14/6875

Abstract

Magnetic moment orientations of α-Fe nanowire arrays with two different diameters have been investigated by means of transmission Mössbauer spectroscopy (MS) and conversion electron Mössbauer spectroscopy (CEMS). From the intensity ratio in the sextets of MS and CEMS, it is found that inside the α-Fe nanowire array (60 nm in diameter) the magnetic moments are well parallel to the nanowires, but near the extremities of the nanowires the magnetic moment orientation deviates from parallelism to the long axis of the wire. When the diameter of the α-Fe nanowires increases (300 nm in diameter), CEM spectra indicate that the mean angle of orientation between the moment direction and the long axis of the wire becomes larger near the extremities of the nanowires. The calculated configurations of magnetic moment orientations are consistent with the MS and CEMS measurements.

1. Introduction

Current interest in studies on ferromagnetic nanowire arrays is stimulated by the potential application to future magnetic recording media. Self-assembled template methods such as anodic aluminum oxide templates (AAOTs) have been employed to prepare nanowire arrays commercially [1–3]. Many magnetic systems including nanowire arrays of Fe, Co, Ni and alloys have been investigated [4–7]. A recent review by Zeng [8] leads to a better understanding of the magnetism of nanowires. However, the methods commonly used to study nanowire arrays only provide the properties of the entire wire or array, and the study of the local properties is still lacking. Due to the detection depth, conversion electron Mössbauer spectroscopy (CEMS) provides a suitable approach to observe the properties near the extremities of Fe nanowires.

[1] Author to whom any correspondence should be addressed.

0953-8984/02/276875+08$30.00

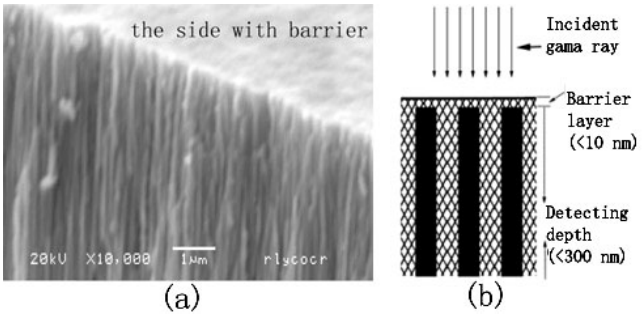

Figure 1. (a) Scanning electron microscopy (SEM) image of a cross section of anodic aluminum oxide containing an Fe nanowire array about 60 nm in diameter. (b) Schematic view of the CEMS measurement; the incident γ-photons are parallel with the nanowires.

For the application of perpendicular magnetic recording, the magnetic moments are expected to be perpendicular to the magnetic recording disc [9]. Since magnetic nanowire arrays embedded in porous AAOTs are considered as good candidates for perpendicular magnetic recording [10], it is necessary to study the magnetic moment orientations in such magnetic nanowire arrays, especially near the extremities, where the array is closer to the head. In this paper, the magnetic moment orientations near the extremities of α-Fe nanowires are studied by means of CEMS. Transmission Mössbauer spectroscopy (MS) is also employed to confirm the magnetization direction of the entire nanowire array. Meanwhile, micromagnetic simulations show that the configurations of magnetic moment orientations are similar to the results of MS and CEMS measurements.

2. Experiment and simulation

The fabrication process of the α-Fe nanowire arrays is similar to those reported earlier [11, 12]. 0.4 mm thick aluminum foil (99.999%) was used for anodic oxidation. At room temperature, Al foil was anodized for 1 h, at 40 V in 0.6 M oxalic acid and at 150 V in 0.1 M phosphoric acid, thus the pores of the templates are about 60 and 300 nm in diameter, respectively. The so-called decreasing voltage method was employed and each anodic voltage was decreased to 7 V step by step. Iron was electrodeposited into the pores of AAOTs by AC electrolysis in an electrolyte containing $FeSO_4{\cdot}7H_2O$ (120 g l^{-1}), boric acid (45 g l^{-1}) at 20 °C, 200 Hz, 12 V AC and for 10 min.

The structures of the α-Fe nanowire arrays were characterized by means of x-ray diffraction (XRD) using a Rigaku D/Max-2400 diffractometer with Cu Kα radiation. The transmission Mössbauer spectrum (MS) was obtained at room temperature using a constant-acceleration spectrometer with a ^{57}Co in Rh source. CEMS measurements were made at room temperature with a gas flow proportional counter (a counter gas with a mixture of 96% helium and 4% methane was used). The γ-ray beam is parallel to the nanowires (figure 1(b)). The integral CEMS involved the detection of all emerging electrons, and the detection depth of CEMS is about 100 nm. The Mössbauer spectral parameters were obtained by fitting Lorentzian line shapes to the experimental data.

The magnetization states can be assessed, especially by the direction dependence of the line intensity in the Mössbauer spectra. In the sextet the intensity ratio is $3 : q{:}1{:}1{:}q{:}3$, where q is the intensity ratio of the second and the fifth peaks, and $q = 4\sin^2\theta/(1+\cos^2\theta) = 4(1-\cos^2\theta)/(1+\cos^2\theta)$. θ is usually the angle between incident γ-photons and the magnetization

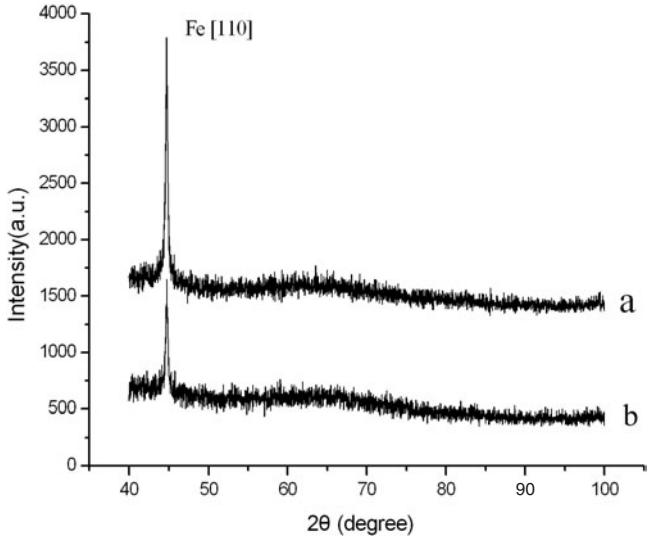

Figure 2. Room-temperature XRD patterns of the Fe nanowire arrays. Patterns were taken from the open side (a) $d = 60$ nm and from the side with the barrier (b) $d = 300$ nm.

direction. When $\theta = 0°$, the intensity ratio q is 0, and $q = 4$ when $\theta = 90°$. If the sample is not uniformly magnetized, an averaging must be performed. The analysis of the intensity ratio can therefore be used to derive $\langle \cos^2 \theta \rangle$ and the mean angle $\langle \theta \rangle$ of orientation, which is between the moment direction and the direction of γ-ray propagation, where $\cos^2\langle\theta\rangle = \langle \cos^2 \theta \rangle$ [13].

In zero magnetic field, the magnetization states for an individual cylindrical Fe nanowire were calculated by a three-dimensional micromagnetic model. The final states originated from the minimization of the total energy density function: $E_{total} = E_{exch} + E_{demag} + E_{anis}$, where E_{exch}, E_{demag} and E_{anis} are the exchange, demagnetization and magnetocrytalline anisotropy energy, respectively. The traditional Landau–Lifshitz–Gilbert equation was solved for each element. All simulations were performed using the OOMMF (object-oriented micromagnetics framework) code from NIST. The OOMMF parameters were the values of bulk iron: $M_s = 1700 \times 10^3$ A m^{-1}, $A = 2.1 \times 10^{-11}$ J m^{-1} and $K_1 = 47.0 \times 10^3$ J m^{-3}. The easy axis of magnetocrytalline anisotropy was along the wire.

3. Results and discussion

As indicated in figure 1(a), the cross-section image taken by SEM shows that the nanowires are 60 nm in diameter and more than 20 μm in length [14]. XRD patterns (figure 2) were obtained from the open side and from the side closed with the barrier layer, indicating that the Fe nanowire arrays are stabilized in bcc structure, and a preferential (110) texture is seen [15].

Figure 3 shows the transmission Mössbauer spectrum of the α-Fe nanowire array (60 nm in diameter), and the incident γ-photons were detected parallel to the long axis of the wire (normal to the membrane). It appears that peaks 2 and 5 almost vanish compared with the background of the spectrum, and the distinct magnetic texture of this α-Fe nanowire array is observed [16]. The corresponding parameters are listed in table 1.

CEMS measurements were performed on the top of the α-Fe nanowire arrays from the side with the barrier (figure 1(b)). The CEM spectra of three samples, which are (a) an α-Fe nanowire array with $d = 60$ nm, (b) an α-Fe nanowire array with $d = 300$ nm and (c) an α-Fe

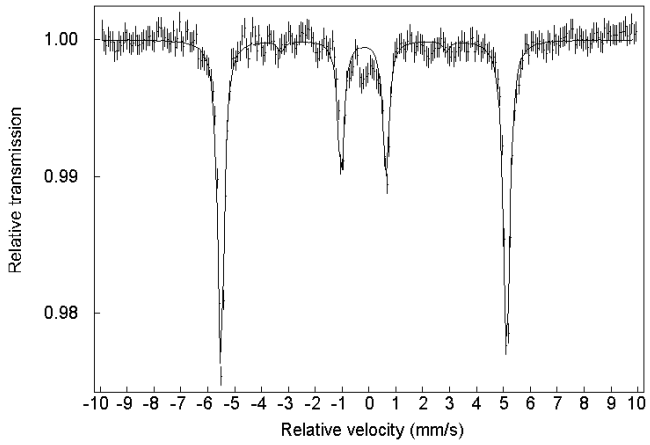

Figure 3. ^{57}Fe Mössbauer spectrum of the α-Fe nanowire array with $d = 60$ nm. The solid curve is the fitting curve.

Table 1. Results of least-squares fitting of MS in figure 3. The linewidth (FWHM), isomer shift (IS), quadrupole shift (2ϵ), hyperfine field (B_{hf}) and the intensity ratio of the second and the fifth peaks (q) are listed. All the parameters are obtained at room temperature.

Sample	FWHM (mm s^{-1})	IS (mm s^{-1})	2ϵ (mm s^{-1})	B_{hf} (T)	q
$d = 60$ nm	0.28	−0.17	0.00	33.1	0.09

Table 2. CEMS fitting results of 60, 300 nm and standard (α-Fe foil) samples. The linewidth (FWHM), isomer shift (IS), quadrupole shift (2ϵ), hyperfine field (B_{hf}) and the intensity ratio of the second and the fifth peaks (q) are obtained at room temperature.

Samples	FWHM (mm s^{-1})	IS (mm s^{-1})	2ϵ (mm s^{-1})	B_{hf} (T)	q
$d = 60$ nm	0.32	−0.17	0.00	33.1	0.27
$d = 300$ nm	0.30	−0.17	0.00	33.1	0.66
Standard α-Fe foil sample	0.26	−0.18	0.00	33.1	3.54

foil 25 μm in thickness, are shown in figure 4. The ratio q is 0.66 for $d = 300$ nm while 0.27 for $d = 60$ nm. The CEMS parameters are given in table 2. Hyperfine fields are similar to that in bulk iron, and the line width is larger for the α-Fe nanowire array with smaller diameter. According to the relation between hyperfine field and magnetization, it is deduced that, near the extremities of nanowires, M_s is the same as that of the bulk iron. In the CEM spectrum of standard α-Fe foil 25 μm in thickness, $q = 3.54$.

As shown in figure 3, the incident γ-ray transmits along the whole nanowire array ($d = 60$ nm); it can be found that peaks 2 and 5 are comparable to the background and have almost disappeared, so $\langle \cos^2 \theta \rangle$ is nicely close to unity and $\langle \theta \rangle$ is almost equal to zero for the entire nanowire array. However, near the extremities, as it is shown in figure 4, CEM spectra obviously indicate the existence of the second and the fifth peaks in the sextet; the calculated $\langle \theta \rangle$ is 21° for $d = 60$ nm. The detection depth of CEMS is about 100 nm [17], comparable to the SEM observation; 100 nm is nearly 1% of the total nanowire. The resonance atoms near the extremities of nanowires therefore have negligible contribution to transmission MS. Therefore in the MS spectrum peaks 2 and 5 mainly originate from the interior resonance atoms of the α-Fe nanowires. Hence this indicates that inside the α-Fe nanowire array ($d = 60$ nm)

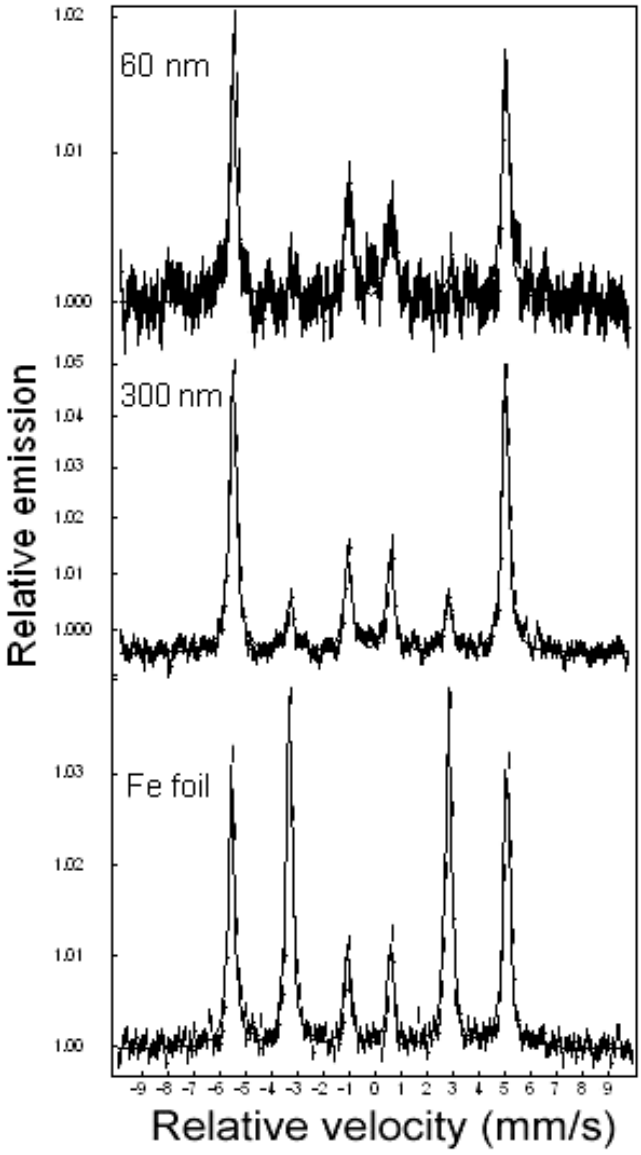

Figure 4. Typical CEMS at RT: the α-Fe nanowire arrays ($d = 60$ and 300 nm), and the α-Fe foil for comparison. The solid curves are the fitting curves.

the magnetic moments are well parallel to the nanowire, but near the extremities the angles between the magnetic moments and the long axis of the wire become larger. When the diameter of the nanowire array increases up to 300 nm, in the CEM spectrum the intensity of peaks 2 and 5 rises and the mean angle $\langle\theta\rangle = 32^\circ$, which is larger than that of $d = 60$ nm.

To obtain more detailed information on magnetic moment orientations in the α-Fe nanowires, we performed micromagnetic simulations of single α-Fe nanowires. The sizes of the simulated cylinders are $d = 60$ nm, $l = 3000$ nm and $d = 300$ nm, $l = 5000$ nm respectively. Micromagnetic simulation of a single nano-cylinder is an effective

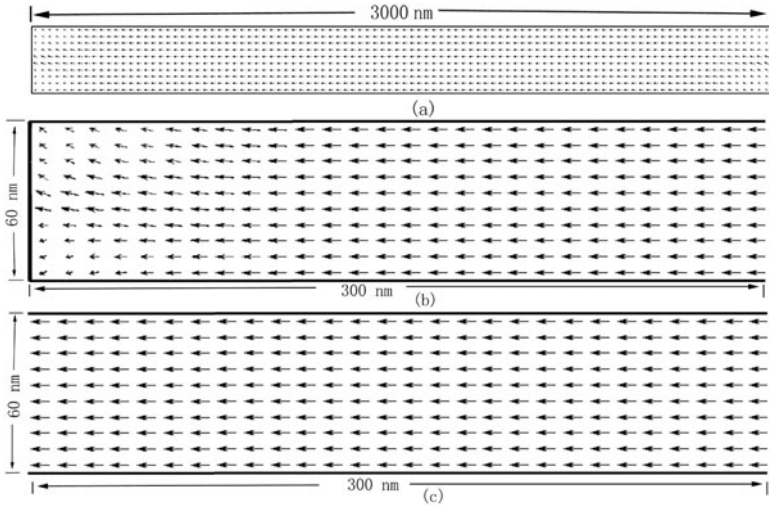

Figure 5. (a) Typical configuration of magnetic moment orientations for a simulated α-Fe wire 60 nm in diameter and 3000 nm in length; (b) and (c) show the configurations at the end and the centre of the wire respectively. Notice that the magnetic moments near the end diverge from the long axis of the wire, while at the centre the moments are mostly oriented along the wire.

approximation [18]. The simulation was accomplished when the equilibrium states were obtained. The magnetic moment orientations in the central vertical section of the cylinder are illustrated in figures 5 and 6. The single nanowire 60 nm in diameter is close to being a single-domain state, i.e. inside the wire the magnetic moments are well parallel to the wire axis, whereas near the extremities the magnetic moments slightly diverge from the long axis of the wire; when the magnetic moment is closer to the top of wire, the diverging angle becomes larger. As the diameter increases up to 300 nm, antiparallel magnetic moments are found and some magnetic moments are perpendicular to the wire at its end, so the angles between moments and the long axis of the wire increase. From the comparison of figures 5 and 6 within 100 nm in depth, it is seen that, at the same distance from the top of wire, the diverging angle of moment is larger for $d = 300$ nm than for $d = 60$ nm, hence so must be the average angle.

The magnetic moment orientations in α-Fe nanowire arrays are mostly predominated by the characteristic cylinder geometry of the nanowires [19]. A high aspect ratio of the wire results in high shape anisotropy, so the magnetic moments are mainly oriented parallel to the nanowire. Therefore, in the MS spectrum, the second and fifth peaks have obviously disappeared for $d = 60$ nm, which is similar to the case in [11]. However, near the extremities, because of the influence of the demagnetization field [12], the magnetic moments diverge from the long axis of the wire. When the size decreases ($d = 60$ nm), the α-Fe nanowires are close to a single-domain state, so even near the extremities the magnetic moments are better oriented along the wire than in the nanowire array with $d = 300$ nm. Micromagnetic simulations provide similar results. For $d = 60$ nm the magnetic moments are well parallel to each other and lie along the wire, and near the extremities there is just a small declination, while for $d = 300$ nm near the end of the wire some magnetic moments are perpendicular to the long axis of wire. Hence, near the extremities, the mean angle of orientation between the moment direction and the long axis of the wire is larger for $d = 300$ nm than for $d = 60$ nm. Then in CEMS measurements, the corresponding second and fifth peaks are lower for $d = 60$ nm than for $d = 300$ nm.

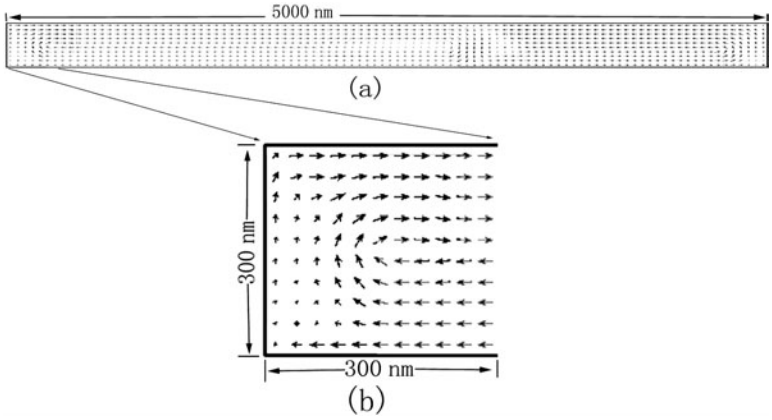

Figure 6. Micromagnetic simulation for the α-Fe wire 300 nm in diameter and 5000 nm in length, (a) total and (b) near the extremity. Some magnetic moments are perpendicular to the wire near the extremity.

4. Conclusion

In summary, transmission MS observation indicates that there is a preferred magnetic orientation along the entire α-Fe nanowire array ($d = 60$ nm). Near the extremities, CEMS measurements reveal that the magnetic moments diverge from the long axis of the wire, and the mean angle of orientation between the moment direction and the long axis of the wire is larger for the α-Fe nanowire array with larger diameter. The magnetic moment orientations of the α-Fe nanowire arrays (inside or near the extremities) are similar to the simulated results.

Acknowledgments

The authors would like to thank Chief Engineer Dakang Song for XRD measurements and Professor Jiazheng Zhao for SEM observation. Spectrum fitting was performed with the help of Rong Shan and Yue Ma. This work is supported by National Natural Science Foundations of China (grant no 19835050).

References

[1] Cheng G S, Zhang L D, Zhu Y, Frei G T, Li L, Mo C M and Mao Y Q 1999 *Appl. Phys. Lett.* **75** 2455
[2] Wang X F, Zhang L D, Shi H Z, Peng X S, Zheng M J, Fang J, Chen J L and Gao B J 2001 *J. Phys. D: Appl. Phys.* **34** 418
[3] Li Y, Meng G W, Zhang L D and Philipp F 2000 *Appl. Phys. Lett.* **76** 2011
[4] Kwon H W, Kim S K and Jeong Y 2000 *J. Appl. Phys.* **87** 7405
[5] Zeng H, Zheng M, Skomski R, Seilmyer D J, Liu Y, Meon L and Bandyopadhyay S 2000 *J. Appl. Phys.* **87** 4718
[6] Strijkers G J, Dalderop J H J, Broeksteeg M A A, Swagten H J M and de Jonge W J M 1999 *J. Appl. Phys.* **86** 5141
[7] Fedosyuk V M, Kasyutich O I and Schwarzacher W 1999 *J. Magn. Magn. Mater.* **199** 246
[8] Zeng H, Skomski R, Menon L, Liu Y, Bandyopadhyay S and Sellmyer D J 2002 *Phys. Rev.* B **65** 134426
[9] Lohau J, Moser A, Rettner C T, Best M E and Terris B D 2001 *Appl. Phys. Lett.* **78** 990
[10] Sun S, Murray C B, Weller D, Folks L and Moser A 2000 *Science* **287** 1989
[11] Peng Yong, Zhang Hao-Li, Pan Shan-Lin and Li Hu-Lin 2000 *J. Appl. Phys.* **87** 7405
[12] Paulus P M, Luis F, Kroll M, Schemid G and De Jongh L J 2001 *J. Magn. Magn. Mater.* **224** 180

[13] Habbal F and Vetterling W T 1984 *J. Appl. Phys.* **55** 2291
[14] Jessensky O, Muller F and Gosele U 1998 *J. Appl. Phys.* **72** 1173
[15] Wang J-B, Liu Q-F, Xue D-S, Peng Y, Cao X-Z and Li F-S 2001 *J. Phys. D: Appl. Phys.* **34** 3442
[16] Greneche J M and Varret F 1982 *J. Phys. C: Solid State Phys.* **15** 5333
[17] Sauer C H 1993 *IFF-Ferienkurs* **29** 1–29
[18] Ferre R, Ounadjela K, Geoge J M, Piraux L and Dubois S 1997 *Phys. Rev.* B **56** 14 066
[19] Cowburn R P and Welland M E 1998 *Phys. Rev.* B **58** 9217